PRACTICAL ELECTRON MICROSCOPY IN MATERIALS SCIENCE

2 Monograph Two

Electron Diffraction in the Electron Microscope

J W Edington

Philips Technical Library

Monographs in Practical Electron Microscopy in Materials Science

2

ELECTRON DIFFRACTION IN THE ELECTRON MICROSCOPE

J. W. EDINGTON

Department of Metallurgy and Materials Science, University of Cambridge, Cambridge, England

SBN 333 18292 8

First published 1975 by
THE MACMILLAN PRESS LTD
London and Basingstoke
Associated companies in New York, Dublin,
Melbourne, Johannesburg and Madras

PHILIPS

Trademarks of Philips' Gloeilampenfabrieken

Filmset at The Universities Press, Belfast, Northern Ireland
Printed by Thomson Litho Ltd., East Kilbride, Scotland

PREFACE

This is the second of a series of monographs on electron microscopy aimed at users of the equipment. They are written both as texts and sources of reference emphasising the applications of electron microscopy to the characterisation of materials.

In some places the author has referred the reader to material appearing in other monographs of the series. The following title has already been published:

1. The Operation and Calibration of the Electron Microscope

and the titles in preparation are:

3. Interpretation of Transmission Electron Micrographs

4. Typical Electron Microscope Investigations

ACKNOWLEDGEMENTS

It is a pleasure to acknowledge Drs L. M. Clareborough, C. P. Cutler, P. Humble, B. Kear, K. N. Melton, P. H. Pumphrey and M. N. Thompson for their useful comments on the manuscript. I would also like to acknowledge the many useful discussions over a number of years with all members of my research group in Cambridge. These formed the basis for many of the sections of this series of monographs. In addition, particular thanks are due to Messrs R. H. Bricknell, J. L. Henshall, D. A. Porter and Dr. D. B. Williams for their help in proof-reading the manuscript. I am also grateful to Professor R. W. K. Honeycombe for his continued advice and encouragement.

I would like to thank the large number of research workers who have provided me with illustrations and tables. They are acknowledged individually in the relevant figure and table captions. I am also grateful to the following journals and publishers for permission to reproduce a number of photographs, tables and figures: *Acta Metallurgica*, *Acta Crystallographica*, *Cambridge Review*, Adam Hilger Ltd, *Journal of Macromolecular Science*, *Journal of Materials Science*, *Journal of Microscopy*, *Journal of Physics F*, *Journal of Physics Radium*, *Journal of the Physical Society of Japan*, McGraw-Hill, *Metallurgical Reviews*, *Metallurgical Transactions*, *Metal Science Journal*, North-Holland Publishing Co., *Philosophical Magazine*, *Physica Status Solidi*, *Proceedings of the Royal Society*, *Transactions Quarterly of the American Society for Metals*, University of California Press.

This series of monographs has been published with the support of the Philips Company of The Netherlands. In particular I would like to thank Mr J. Fay of that organisation for his unfailing enthusiasm and encouragement.

CONTENTS

PART III. USES OF DIFFRACTION PATTERNS FROM SINGLE CRYSTALS: THE BASIC DIFFRACTION PATTERN 30

PART IV. USES OF DIFFRACTION PATTERNS FROM SINGLE CRYSTALS: THE FINE STRUCTURE IN THE PATTERN 59

2. ELECTRON DIFFRACTION IN THE ELECTRON MICROSCOPE

Electron diffraction patterns are routinely obtained in the electron microscope and are used to gain quantitative information on the following.

(1) The identity of phases and their orientation relationship to the matrix.

(2) Habit planes of precipitates, slip planes in materials.

(3) Exact crystallographic descriptions of crystal defects produced by deformation, irradiation, etc.

(4) Order/disorder, spinodal decomposition, magnetic domains and similar phenomena.

The first part of this chapter contains those features of the kinematical diffraction theory necessary to interpret diffraction patterns obtained from the electron microscope. The second, third and fourth parts are devoted to indexing diffraction patterns and to their use in metallurgical investigations. In this monograph, all important stereograms are printed to fit the standard Institute of Physics 5 inch stereographic net so that it is possible to work through examples.

PART I. INTRODUCTION TO ELECTRON DIFFRACTION

2.1 General Introduction

Electrons may be regarded as particle waves with wavelength λ given by the de Broglie relation $mv = h/\lambda$. If the electron is accelerated to a voltage V_c, the relativistically corrected wavelength is

$$\lambda = \frac{h}{\{2mV_c e(1 + eV_c/2mc^2)\}^{1/2}} \tag{2.1}$$

where h is Planck's constant, m is the mass of the electron, e is its charge and c is the velocity of light. Values of λ for different accelerating voltages obtained from the above equation are tabulated in appendix 7. At 100 kV, the conventional accelerating voltage for transmission electron microscopy, the relativistically corrected wavelength is 3.7×10^{-3} nm.

In transmission electron microscopy a monochromatic beam of electrons is accelerated through a thin specimen which is usually a single crystal 0.1–0.5 μm thick. On the exit side of the specimen several diffracted beams are present in addition to the transmitted beam, and these are focussed by the objective lens to form a spot pattern in its back focal plane in the manner shown in figure 1.10(a). As explained in section 1.5, this diffraction pattern is magnified by the other lenses to produce a spot pattern, such as that shown in figure 2.1, on the viewing screen. In this case the incident beam direction $\boldsymbol{B}$ is [100] in an aluminium (face-centred cubic, f.c.c.) single-crystal specimen. The transmitted beam is marked T and the arrangement of diffracted beams D around the transmitted beam is characteristic of the four-fold symmetry of the [100] cube axis of aluminium. Here physical and mathematical descriptions of the diffraction process are given, to demonstrate both why diffraction patterns such as that in figure 2.1 occur, and how they may be interpreted using simple geometrical concepts.

2.2 A Geometrical Approach to Electron Diffraction from a Crystalline Specimen

When a beam of electrons is incident on the top surface of a thin crystalline electron microscope specimen, specific diffracted beams arise at the bottom exit surface. Although each individual atom in the crystal scatters the incident beam, the scattered wavelets will only be in phase (that is reinforce) in particular crystallographic directions. Thus diffraction may be discussed in terms of the phase relationships between the scattered waves from each atom in the crystal.

2.2.1 *Scattering by an Individual Atom*

The scattering process at an atom is shown schematically in figure 2.2. Here a plane wave is incident on an atom A which acts as a source for a spherical wave propagating at an angle 2θ relative to the incident wave direction. The efficiency of the atom in scattering waves is described in terms of the atomic scattering factor f_θ which depends on both scattering angle θ and incident electron wavelength λ. The term f_θ is defined as

$$f_\theta = \frac{\text{amplitude scattered through angle } 2\theta \text{ by the atom}}{\text{amplitude scattered through angle } 2\theta \text{ by a single electron}}$$

and is given by

$$f_\theta = \frac{me^2}{2h^2}\left(\frac{\lambda}{\sin\theta}\right)^2 (Z - f_x) \tag{2.2}$$

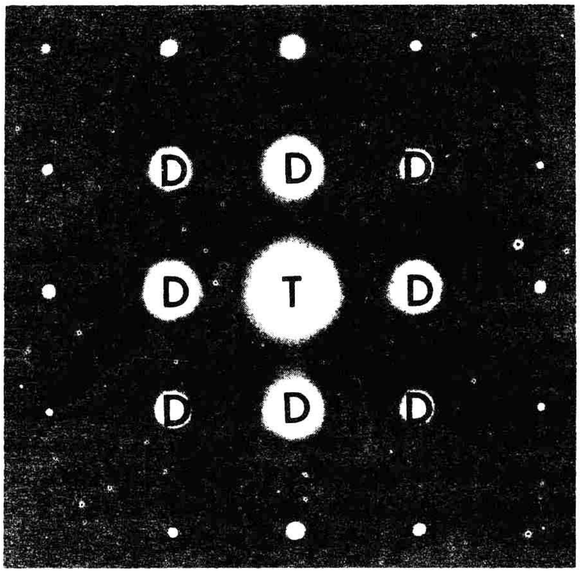

Figure 2.1 A typical spot pattern from an aluminium (f.c.c.) single crystal specimen, incident beam direction $\boldsymbol{B}$ = [100]. T, transmitted spot; D, diffracted spot

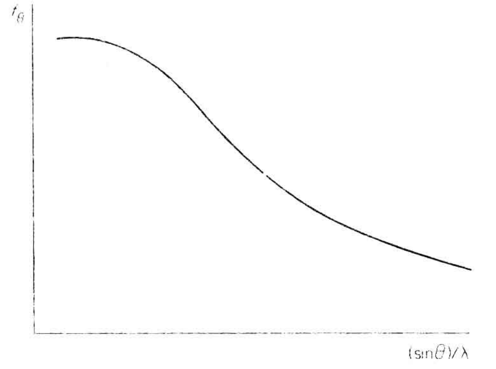

Figure 2.3 A schematic diagram showing the variation of the atomic scattering factor f_θ with (sin θ)/λ

where Z is the atomic number, f_x is the atomic scattering factor for x-rays and the remaining symbols are those defined previously.

The atomic scattering factor increases with increasing atomic number and is normally expressed as a function of (sin θ)/λ (see appendix 8). The general form of the relationship is shown schematically in figure 2.3.

2.2.2 *Scattering by a Crystal*

Before considering diffraction by a regular three-dimensional array of atoms, the principles involved are discussed by analogy with the diffraction of monochromatic light by a grating, see figure 2.4. In this diagram there is a set of slits consisting of plates that are infinitely long, perpendicular to the paper and have spacing a. A screen is placed at a large distance R from the grating and we consider the situation at a point X. If the waves scattered from openings 1 and 2 are in phase, that is their path difference PD is an integral multiple of their wavelength λ, X will be bright. Two in-phase waves are shown in figure 2.4 arriving at X. However, at other points on the screen, the path difference may be such that the waves are out of phase and the total intensity is very low or zero. When this interference process is considered over the whole screen, alternate bright and dark lines are obtained running perpendicular to the paper with the approximate intensity distribution shown in figure 2.4. As α increases the intensity of the fringes decreases because the efficiency for scattering through large angles is lower. In the case of a three-dimensional crystal, a similar path difference argument shows that the diffraction of the monochromatic electron beam by the regularly spaced three-dimensional array of atoms gives an interference pattern of beams, instead of lines.

The theoretical treatment of electron diffraction patterns generally relies on the kinematical theory of electron diffraction and the following assumptions.

(1) The incident beam is monochromatic, that is the electrons all have the same energy and wavelength.

(2) The crystal is free from distortion.

(3) Only a negligible fraction of the incident beam is scattered by the crystal, that is every atom

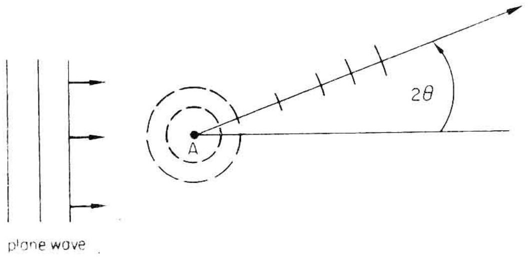

Figure 2.2 The scattering of a plane wave at an atom A through the formation of spherical wavelets travelling at an angle 2θ to the original direction of motion

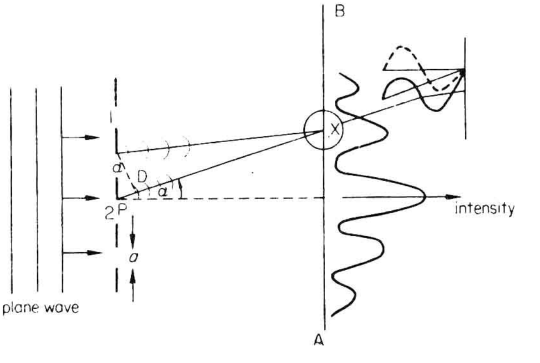

Figure 2.4 Diffraction of monochromatic light by a line grating. Inset shows waves arriving at X in phase

in the crystal receives an incident wave of the same amplitude.

(4) The incident and scattered waves may be treated as plane waves.

(5) There is no attenuation of the electron beam with increasing depth in the crystal, that is no absorption.

(6) There is no interaction between the incident beam and the scattered wavelets, that is the refractive index of the crystal is unity.

(7) There is no re-scattering of scattered waves.

In the electron microscope, the above assumptions are not in general true. Nevertheless, the kinematical approach is still satisfactory for a general description of *diffraction patterns*. In contrast, as we shall see in section 3, it is necessary to use the more realistic dynamical theory of electron diffraction to interpret the details of most *images* obtained in the electron microscope.

2.2.2.1 *The Bragg law*

The above treatment of diffraction introduced the important point that strong diffracted beams arise because scattered wavelets are in phase in particular directions in the crystal, that is the path difference is an integral number of wavelengths. This leads directly to a particularly simple method of visualising diffraction by a crystal, known as the Bragg law. Figure 2.5(a) depicts the situation describing diffraction in terms of the Bragg law for a transmitting thin electron microscope specimen ~ 1000–3000 Å thick. Consider the particular case when the incident beam is made up of plane waves in phase and oriented at an angle θ relative to two (hkl) crystal planes I and II. Let the two waves be reflected by these crystal planes at an angle θ. At the plane wavefront CD two situations may occur.

(1) The two waves may be in phase, as shown in figure 2.5(a), in which case reinforcement will occur and a strong reflected beam will be present.

(2) The waves may be out of phase, that is they will interfere and there will be either zero or a very weak reflected beam.

Case (1), that is a strong beam, will occur if the path difference POD is an integral number of wavelengths $n\lambda$. Since PD = OD = OL $\sin\theta$, $2\text{OL}\sin\theta = n\lambda$ for a strong beam. However, OL is the interplanar spacing $d_{(hkl)}$. Thus, for a strong reflection, we must have

$$2d_{(hkl)}\sin\theta = n\lambda \qquad (2.3)$$

which is known as the Bragg law. In effect we have shown that there will be a strong diffracted beam on the exit side of the crystal only if there is a set of crystal planes oriented at a critical angle θ relative to the incoming beam. For the present we may

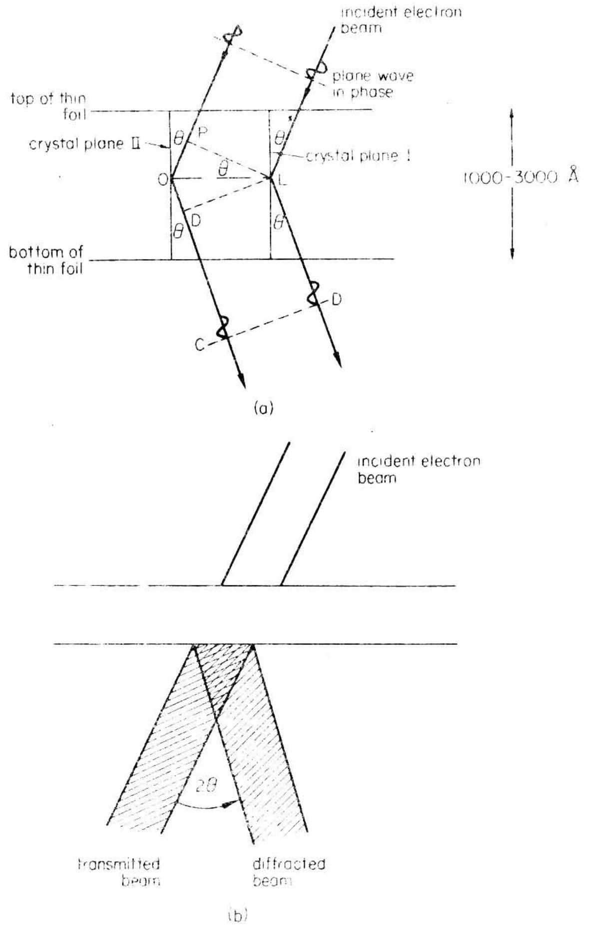

Figure 2.5 (a) Reflection at the Bragg angle θ from crystal planes in a thin foil electron microscope specimen. (b) The relationship between incident, transmitted and diffracted beams for a transmitting specimen

postulate that the reflective process is inefficient and that some of the electrons are not reflected but pass straight through the crystal. Thus there will be both a transmitted and a reflected beam at the bottom surface of the crystal with an angular relation 2θ (see figure 2.5(b)). In terms of the Bragg law the diffracted beams are referred to as reflected beams.

2.2.2.2 *The Laue conditions*

As an alternative to the above approach, diffraction may be considered in terms of scattering by individual atoms. This approach has the advantage that it may be used more quantitatively to describe diffraction in terms of the reciprocal lattice. Figure 2.6(a) shows this case for atoms O and L where the position of L relative to the origin O may be described in terms of a vector $\boldsymbol{r}$. The incident and scattered waves are now described in terms of the unit vectors $\boldsymbol{p}_0$ and $\boldsymbol{p}$, respectively. Again the scattered waves will be in phase if the path difference POD is an integral number of wavelengths. We may write the distance PO in

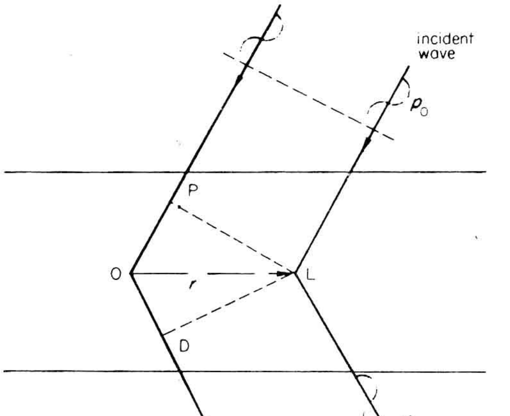

Figure 2.6 (a) The additive scattering from atoms situated at O and L in a thin foil specimen. (b) The vector diagram describing the scattering process

vector notation as $\boldsymbol{r} \cdot \boldsymbol{p}_0$ and OD as $\boldsymbol{r} \cdot \boldsymbol{p}$, that is $\mathrm{POD} = \boldsymbol{r} \cdot \boldsymbol{p} - \boldsymbol{r} \cdot \boldsymbol{p}_0 = \boldsymbol{r} \cdot (\boldsymbol{p} - \boldsymbol{p}_0)$. Defining a scattering vector $\boldsymbol{P} = \boldsymbol{p} - \boldsymbol{p}_0$ we have

$$\mathrm{POD} = \boldsymbol{r} \cdot \boldsymbol{P} = n\lambda \tag{2.4}$$

The relationship between $\boldsymbol{p}$, $\boldsymbol{p}_0$ and $\boldsymbol{P}$ may be described in terms of the vector triangle shown in figure 2.6(b) in which all vectors have been normalised by dividing by the wavelength λ.

It is convenient to describe the position of each atom relative to the x, y and z crystal axes instead of the simple vector $\boldsymbol{r}$. Thus we may resolve $\boldsymbol{r} \cdot \boldsymbol{P}$ into the components $\boldsymbol{P} \cdot \boldsymbol{a}$, $\boldsymbol{P} \cdot \boldsymbol{b}$ and $\boldsymbol{P} \cdot \boldsymbol{c}$ where $\boldsymbol{a}$, $\boldsymbol{b}$ and $\boldsymbol{c}$ are the repeat distances of the atoms along the crystal axes. Each of these resolved components must also be integral values of λ and we may express equation (2.4) as

$$\begin{aligned} \boldsymbol{P} \cdot \boldsymbol{a} &= h\lambda \\ \boldsymbol{P} \cdot \boldsymbol{b} &= k\lambda \\ \boldsymbol{P} \cdot \boldsymbol{c} &= l\lambda \end{aligned} \tag{2.5}$$

where h, k and l are integers. Equations (2.5) are known as the Laue conditions which must be satisfied for strong diffraction to occur and are equivalent to the Bragg law.

2.2.3 *The Reciprocal Lattice*

The reciprocal lattice is important because it may be used as a tool in conjunction with the Ewald sphere construction to simplify considerably the interpretation of electron diffraction patterns as described in section 2.2.4. The reciprocal lattice derives directly from the Laue conditions described in equation (2.5), because their solution is

$$\boldsymbol{P}/\lambda = h\boldsymbol{a}^* + k\boldsymbol{b}^* + l\boldsymbol{c}^* \tag{2.6}$$

where $\boldsymbol{a}^*$, $\boldsymbol{b}^*$ and $\boldsymbol{c}^*$ are vectors defined such that $\boldsymbol{a} \cdot \boldsymbol{a}^* = \boldsymbol{b} \cdot \boldsymbol{b}^* = \boldsymbol{c} \cdot \boldsymbol{c}^* = 1$ and $\boldsymbol{a}^* \cdot \boldsymbol{b} = \boldsymbol{b}^* \cdot \boldsymbol{a}$, etc. $= 0$. Equation (2.6) may be shown to be the solution of equations (2.5) because forming the scalar product of (2.6) with $\boldsymbol{a}$ we have $\boldsymbol{P} \cdot \boldsymbol{a} = h\lambda$, the first Laue condition.

The conditions $\boldsymbol{a} \cdot \boldsymbol{a}^* = 1$ and $\boldsymbol{a} \cdot \boldsymbol{b}^* = 0$, etc., have a simple physical explanation. The relation $\boldsymbol{a}^* \cdot \boldsymbol{b} = \boldsymbol{a}^* \cdot \boldsymbol{c} = 0$ simply means that $\boldsymbol{a}^*$ is perpendicular to $\boldsymbol{b}$ and $\boldsymbol{c}$ and, by a similar argument, $\boldsymbol{b}^*$ is perpendicular to $\boldsymbol{a}$ and $\boldsymbol{c}$ while $\boldsymbol{c}^*$ is perpendicular to $\boldsymbol{a}$ and $\boldsymbol{b}$. This situation is depicted for non-orthogonal axes in figure 2.7. In practice, for crystal structures with orthogonal axes, that is cubic, tetragonal, orthorhombic, the axes of the reciprocal lattice coincide with the crystal lattice. The relations $\boldsymbol{a}^* \cdot \boldsymbol{a} = 1$, etc., define the magnitudes of the vectors as $|\boldsymbol{a}^*| = 1/|\boldsymbol{a}|$ which is the origin of the term reciprocal lattice.

The reciprocal lattice has the following two properties.

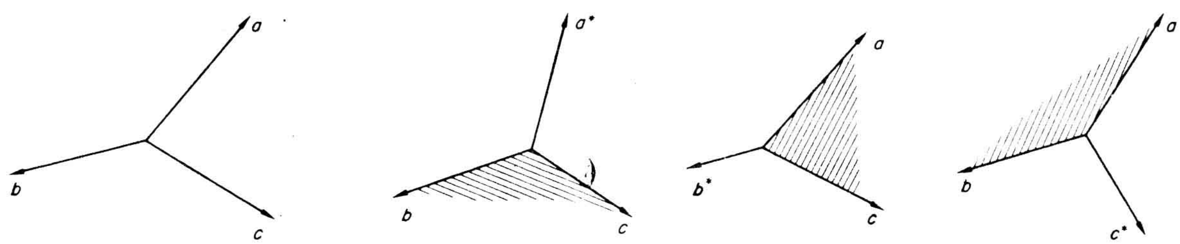

Figure 2.7 The geometrical relationships between the reciprocal lattice vectors $\boldsymbol{a}^*$, $\boldsymbol{b}^*$, $\boldsymbol{c}^*$ and the real lattice vectors $\boldsymbol{a}$, $\boldsymbol{b}$, $\boldsymbol{c}$

(1) The vector $g_{(hkl)}$ to the point (hkl) of the reciprocal lattice is normal to the plane (hkl) of the crystal lattice.

(2) The magnitude of $g_{(hkl)}$ is $1/d_{(hkl)}$ where $d_{(hkl)}$ is the interplanar spacing of the family of (hkl) planes (see appendix 1).

The first point may be proved with reference to figure 2.8 which shows the (hkl) plane in the crystal cutting the crystal axes at A, B, C. Then from the definition of Miller indices (appendix 1) the (hkl) plane intersects the axes at distances a/h, b/k and c/l. Consider the vector **AB**.

$$\frac{\boldsymbol{a}}{h} + \mathbf{AB} = \frac{\boldsymbol{b}}{k}, \qquad \text{that is } \mathbf{AB} = \frac{\boldsymbol{b}}{k} - \frac{\boldsymbol{g}}{h}$$

The scalar product $\boldsymbol{g} . \mathbf{AB}$ will be zero if $\boldsymbol{g}$ is perpendicular to **AB**.

$$\boldsymbol{g} . \mathbf{AB} = (h\boldsymbol{a}^* + k\boldsymbol{b}^* + l\boldsymbol{c}^*) \cdot \left(\frac{\boldsymbol{b}}{k} - \frac{\boldsymbol{g}}{h}\right)$$

Evaluating with the aid of $\boldsymbol{a} . \boldsymbol{a}^* = 1$, $\boldsymbol{a}^* . \boldsymbol{b} = 0$, etc., we find $\boldsymbol{g} . \mathbf{AB} = 0$. Because this product is zero, $\boldsymbol{g}$ must be normal to **AB**. Similarly it may be shown that $\boldsymbol{g}$ is normal to **AC**. Consequently, because $\boldsymbol{g}$ is normal to two vectors in the plane (hkl), it is normal to the plane itself.

To prove the reciprocal relation between $\boldsymbol{g}$ and d, let $\boldsymbol{n}$ be a unit vector in the direction of $\boldsymbol{g}$.

$$d = \text{ON} = \frac{\boldsymbol{a}}{h} \cdot \boldsymbol{n}$$

But

$$\boldsymbol{n} = \frac{\boldsymbol{g}}{|\boldsymbol{g}|}$$

$$d = \frac{\boldsymbol{a}}{h} \cdot \frac{\boldsymbol{g}}{|\boldsymbol{g}|} = \frac{\boldsymbol{a}}{h} \cdot \frac{(h\boldsymbol{a}^* + k\boldsymbol{b}^* + l\boldsymbol{c}^*)}{|\boldsymbol{g}|} = \frac{1}{|\boldsymbol{g}|}$$

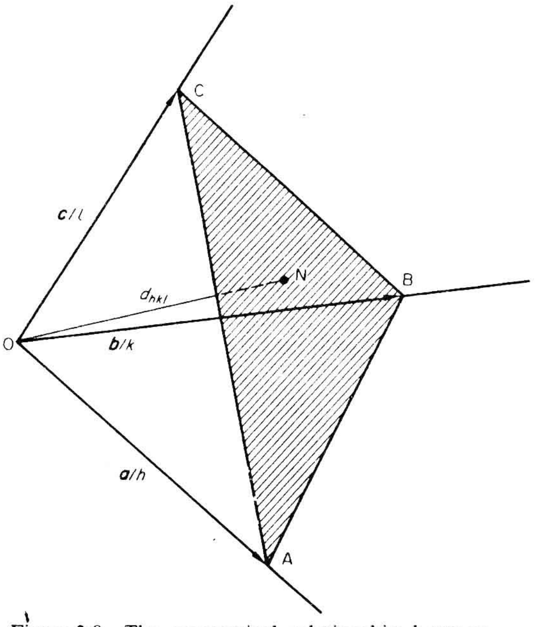

Figure 2.8 The geometrical relationship between the plane normal and $\boldsymbol{g}$

† From this point $\boldsymbol{g}_{(hkl)}$ is abbreviated as $\boldsymbol{g}$.

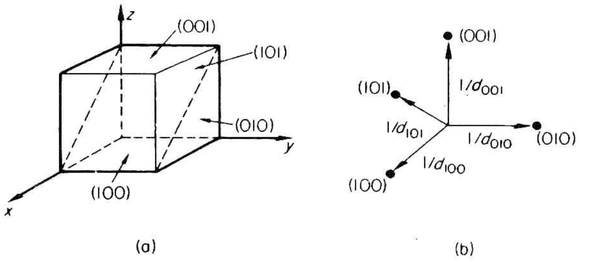

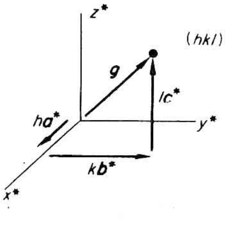

Figure 2.9 The relationship between (a) crystal planes, (b) equivalent reciprocal lattice points and (c) the geometric description of equation (2.7)

Thus we have defined the reciprocal lattice as an array of points, each point corresponding to a particular (hkl) plane and defined by a vector described by points (1) and (2) above. Figure 2.9 shows this relationship between planes in the real lattice and points in the reciprocal lattice for a cubic crystal structure. Each point is labelled with the particular (hkl) indices of the corresponding reflecting plane. Note that a point (hkl) in reciprocal space (figure 2.9(c)) is defined by the steps $h\boldsymbol{a}^*$ along the x axis, $k\boldsymbol{b}^*$ along the y axis and $l\boldsymbol{c}^*$ along the z axis. Thus, as shown in figure 2.9(c),†

$$\boldsymbol{g}_{(hkl)} = h\boldsymbol{a}^* + k\boldsymbol{b}^* + l\boldsymbol{c}^* \qquad (2.7)$$

2.2.4 *The Reciprocal Lattice and Diffraction by a Single Crystal*

The process of diffraction using the Bragg law may be readily visualised in terms of the reciprocal lattice and the Ewald sphere construction. Referring to figure 2.6(b) we have described the Bragg law in terms of a vector triangle. Equation (2.6) describes the base of this triangle in terms of the reciprocal lattice vectors $\boldsymbol{a}^*$, $\boldsymbol{b}^*$, $\boldsymbol{c}^*$, that is $\boldsymbol{P}/\lambda$, and equation (2.7) defines the position of an (hkl) reciprocal lattice point in the same terms. Thus $\boldsymbol{P}/\lambda = \boldsymbol{g}$ defines the reciprocal lattice point.

The significance of this fact may be made clear with reference to figure 2.10 in which a thin single-crystal electron microscope specimen is oriented in the electron microscope to produce reflection from only one set of (hkl) planes. Assuming a unit incident wave vector, that is

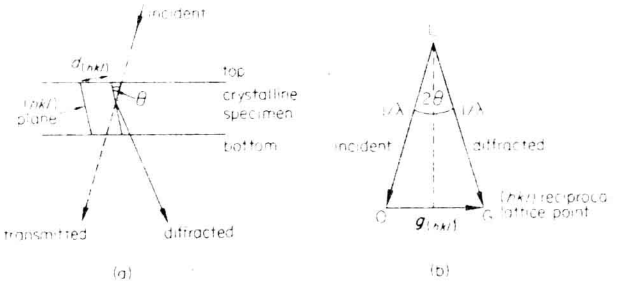

Figure 2.10 (a) Reflection by a set of (hkl) crystal planes, and (b) the vector diagram in reciprocal space describing the same process

$p_0 = p = 1$, the direction of the diffracted beam may be obtained by constructing the following.

(1) A line in the direction of the incident beam and with magnitude $1/\lambda$ running from a point L in the reciprocal lattice to the origin of the reciprocal lattice.

(2) A line LG of the same magnitude $1/\lambda$ from L to the reciprocal lattice point G described by the vector $\boldsymbol{g}_{(hkl)}$ for the particular (hkl) reflecting plane.

In this way, we have reproduced the vector diagram in figure 2.6(b) which describes the Bragg law and have defined the direction of the diffracted beam. Because the reciprocal lattice is three-dimensional and LO and LG are both equal to $1/\lambda$, the construction in figure 2.10(b) represents a small part of a sphere radius $1/\lambda$ in reciprocal space, known as the Ewald or reflecting sphere with centre defined by (1) above. The Ewald sphere construction in the reciprocal lattice is extremely important because it immediately and simply describes the form of the diffraction pattern for a given incident beam direction in the crystal, see section 2.4 for further discussion.

2.3 A Quantitative Approach to Diffraction from a Crystalline Specimen

2.3.1 *The Structure Factor*

The structure factor describes the contribution of the entire unit cell to the diffracted intensity. Up to this point diffraction has been considered in geometric terms and both the position of atoms in the reflecting plane and atomic identity have been ignored. The structure factor enables both of these factors to be included in the description of the diffraction process, and leads to either systematic absence of reflections or differences in intensity from one (hkl) reflection to another.

A physical picture describing the importance of both atomic position and identity is presented in figure 2.11 in terms of the Bragg law. The first-order reflection which might be expected from a cubic crystal structure is $\{001\}$. For such a first-order reflection $n = 1$ and a path difference of λ would occur for waves reflected from successive (001) planes A in figure 2.11(a). However, waves will also be reflected from the layer of atoms (B plane) situated halfway between the (001) planes. Because these are $\lambda/2$ out of phase with those from the A planes destructive interference will occur and the overall reflected intensity will be zero. Consequently for a body-centred cubic (b.c.c.) crystal structure $\{001\}$ reflections are absent. Figure 2.11(b) shows that second-order reflections from (002) planes will be present because the path difference between the A planes will be 2λ and there is complete reinforcement with wave's reflection from B planes which have a path difference of λ. Similar reasoning shows that the first-order (111) reflection is absent for the b.c.c. crystal structure whereas the (222) reflection is present. Consideration of systematic absences from other reflecting planes enables a rule to be formulated which states that, for this crystal structure, if $h + k + l$ is odd, then the reflection is absent.

Scattering from a unit cell may be expressed more rigorously in terms of atomic scattering factors and a path difference argument applied to scattering by each atom within it. This enables the structure factor F defined as

$$F = \frac{\text{amplitude of the wave scattered by all the atoms of a unit cell}}{\text{amplitude of wave scattered by an electron}}$$

to be calculated.

Consider the position of the nth atom in the unit cell in figure 2.12. The vector $\boldsymbol{r}_n$ defines the

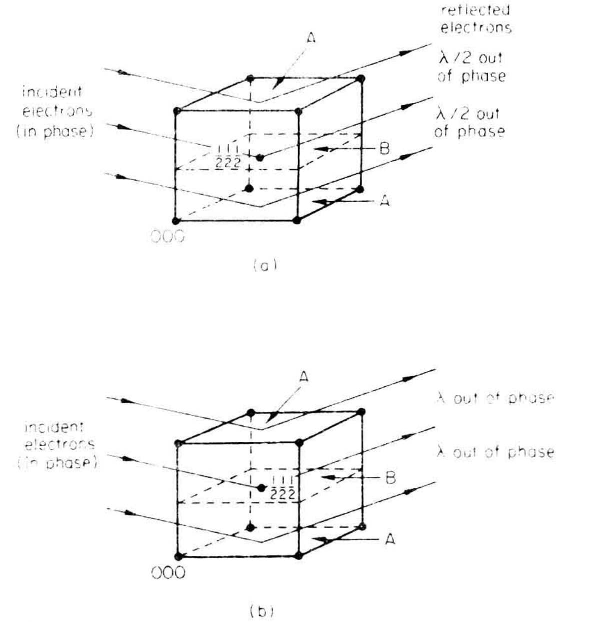

Figure 2.11 The phase relationships for reflection by the layers of atoms shown for (a) (001) and (b) (002) reflections in a b.c.c. crystal structure

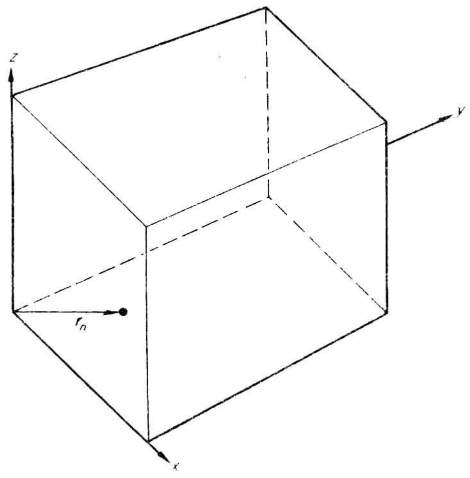

Figure 2.12 The *n*th atom in the unit cell

position of the atom in terms of the fractions x_1, y_1, z_1 of the unit vectors *a*, *b*, *c* along the *x*, *y*, *z* axes as

$$\boldsymbol{r}_n = x_1\boldsymbol{a} + y_1\boldsymbol{b} + z_1\boldsymbol{c} \qquad (2.8)$$

The path difference between an atom at the origin of the unit cell and the *n*th atom is $(\boldsymbol{r}_n \cdot \boldsymbol{P})$ and the resultant phase difference $\phi = 2\pi/\lambda \times$ path difference, that is

$$\phi = k\boldsymbol{r}_n \cdot \boldsymbol{P}$$

where $k = 2\pi/\lambda$.

The structure factor *F* is the sum of the scattered amplitudes of the individual atoms f_n and all the phase differences arising from all path differences, that is

$$F = \sum_n f_n \exp(\mathrm{i}\phi_n) = \sum_n f_n \exp(\mathrm{i}k\boldsymbol{r}_n \cdot \boldsymbol{P}) \qquad (2.9)$$

Substituting equations (2.6), (2.8) for $\boldsymbol{r}_n$ and $\boldsymbol{P}$ we have

$$\boldsymbol{r}_n \cdot \boldsymbol{P} = \lambda(hx_1 + ky_1 + lz_1)$$

that is

$$F_{hkl} = \sum_n f_n \exp\{2\pi\mathrm{i}(hx_1 + ky_1 + lz_1)\} \qquad (2.10)$$

The presence or absence of reflections in the b.c.c. crystal structure can be obtained mathematically from the above structure factor equation as follows.

Intensity of diffracted beam is proportional to

$$|F|^2 = [f_1 \cos\{2\pi(hx_1 + ky_1 + lz_1)\} + f_2 \cos\{2\pi(hx_2 + ky_2 + lz_2)\} + \ldots]^2 + [f_1 \sin\{2\pi(hx_1 + ky_1 + lz_1)\} + f_2 \sin\{2\pi(hx_2 + ky_2 + lz_2)\} + \ldots]^2$$

that is

$$|F|^2 = \sum_i f_i \cos\{2\pi(hx_1 + ky_1 + lz_1)\} + \sum_i f_i \sin\{2\pi(hx_1 + ky_1 + lz_1)\} \qquad (2.11)$$

For b.c.c. metals there are identical atoms at coordinates 000 and $\frac{1}{2}\frac{1}{2}\frac{1}{2}$ in the unit cell as shown in figure 2.11. Thus the intensity

$$I \propto f^2\left[\cos(2\pi \cdot 0) + \cos\left\{2\pi\left(\frac{h}{2} + \frac{k}{2} + \frac{l}{2}\right)\right\}\right]^2 + f^2\left[\sin(2\pi \cdot 0) + \sin\left\{2\pi\left(\frac{h}{2} + \frac{k}{2} + \frac{l}{2}\right)\right\}\right]^2 \qquad (2.12)$$

$$I \propto f^2[1 + \cos\{\pi(h + k + l)\}]^2 + f^2[\sin\{2\pi(h + k + l)\}]^2 \qquad (2.13)$$

that is $I = 0$ if $h + k + l$ is odd, as pointed out earlier in this section.

If the above argument is applied to an ordered intermetallic compound with the B_2 structure such as NiAl, the atom at 000 will be Ni and that at $\frac{1}{2}\frac{1}{2}\frac{1}{2}$ will be Al. Consequently, since the atomic scattering factors are *not* the same, the diffracted intensity is

$$I \propto [f_{Ni} + f_{Al}\cos\{\pi(h + k + l)\}]^2 + [f_{Al}\sin\{\pi(h + k + l)\}]^2 \qquad (2.14)$$

that is

$$I \propto (f_{Ni} + f_{Al})^2 \text{ when } h + k + l \text{ is even}$$

and

$$I \propto (f_{Ni} - f_{Al})^2 \text{ when } h + k + l \text{ is odd}$$

Thus {001} reflections will occur with an intensity proportional to the *difference* in scattering factors of the atoms in the material and are generally less intense than the fundamental reflections. Such reflections are known as superlattice reflections and may or may not be present for the same superlattice depending upon the difference in atomic scattering factor (that is atomic number) of the constituent atoms. Table 2.1 shows structure factor information in relation to the absence of reflections in specific crystal structures. A detailed description of structure factors for all crystal structures will be found in the *International Tables for X-ray Crystallography* (1962).

A physical picture describing the occurrence of superlattice reflections may be obtained from figure 2.11(a). The atoms in the B plane would be

Table 2.1 Structure factor effects

Structure	Reflections absent if
simple cubic	all present
f.c.c. (Al, Cu, etc.)	*h*, *k*, *l*, mixed odd and even
b.c.c. (V, W, α-Fe)	$h + k + l$ odd
c.p.h. (α-Ti, Zr, Mg)	$h + 2k = 3n$ and *l* is odd
b.c.t. (martensite α-Fe)	$h + k + l$ odd
zinc blende (complex cubic) ZnS	*h*, *k*, *l*, mixed odd and even
sodium chloride NaCl	*h*, *k*, *l*, mixed odd and even
diamond (Si, Ge)	*h*, *k*, *l* all even and $h + k + l$ not divisible by four, or *h*, *k*, *l* mixed odd and even

f.c.c., face-centred cubic; b.c.c., body-centred cubic; c.p.h., close-packed hexagonal; b.c.t., body-centred tetragonal.

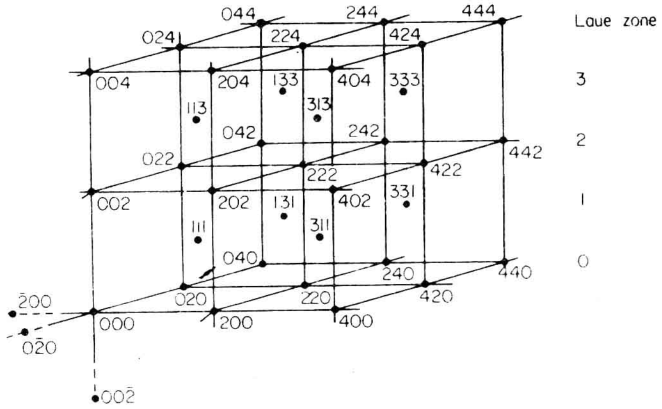

Figure 2.13 The reciprocal lattice for f.c.c. crystal structures

different from those in the A planes and, although the waves interfere as shown before, their intensities are not equal. Consequently a weak (001) superlattice reflection will occur with an intensity depending upon the difference in atomic scattering factors of the constituent atoms, as pointed out before.

It is important to relate the results of these structure factor calculations to the reciprocal lattice. In effect, if the structure factor is zero, the reciprocal lattice point is removed because no reflection will be present in any diffraction pattern. Thus, using the selection rules in table 2.1 for all f.c.c. crystals, the reciprocal lattice is b.c.c. and may be indexed as shown in figure 2.13. For a b.c.c. crystal the reciprocal lattice is f.c.c.

2.3.2 *The Intensity Distribution in Reciprocal Space*

After having considered the influence on diffracted intensity of atomic position and identity within the unit cell, it is necessary to consider the diffracted intensity from the large array of unit cells that go to make up the electron microscope specimen. Figure 2.14(a) shows a thin electron microscope specimen made up of $N_x N_y N_z$ unit cells along the x, y and z axes. The position of the nth unit cell relative to the origin may be defined by the vector $\boldsymbol{r} = n_x\boldsymbol{a} + n_y\boldsymbol{b} + n_z\boldsymbol{c}$ where $\boldsymbol{a}, \boldsymbol{b}, \boldsymbol{c}$ are unit vectors along x, y, z respectively.

Thus, if F is the structure factor of each (identical) unit cell the total scattered amplitude A is the sum of all the phase differences $\phi = k\boldsymbol{a} \cdot \boldsymbol{P}$ along the x, y and z axes for N_x, N_y and N_z unit cells, that is

$$A = F \sum_{n_x=0}^{n_x=N_x-1} \exp(ikn_x\boldsymbol{a} \cdot \boldsymbol{P}) \times \sum_{n_y=0}^{n_y=N_y-1} \exp(ikn_y\boldsymbol{b} \cdot \boldsymbol{P}) \times \sum_{n_z=0}^{n_z=N_z-1} \exp(ikn_z\boldsymbol{c} \cdot \boldsymbol{P}) \qquad (2.15)$$

Each of these terms is a geometric progression of the form

$$\sum_{m=0}^{m=N-1} X^m = X^0 + X^1 + X^2 \ldots X^n \ldots X^{N-1} = \frac{1 - X^n}{1 - X} \qquad (2.16)$$

Thus the first part of equation (2.15) may be written

$$\sum_{n_x=0}^{n_x=N_x-1} \frac{1 - \exp(ikN_x\boldsymbol{a} \cdot \boldsymbol{P})}{1 - \exp(ik\boldsymbol{a} \cdot \boldsymbol{P})} \qquad (2.17)$$

Multiplying equation (2.17) by its complex conjugate

$$|\Sigma|^2 = \frac{1 - \cos(kN_x\boldsymbol{a} \cdot \boldsymbol{P})}{1 - \cos(k\boldsymbol{a} \cdot \boldsymbol{P})} = \frac{\sin^2(\frac{1}{2}N_x k\boldsymbol{a} \cdot \boldsymbol{P})}{\sin^2(\frac{1}{2}k\boldsymbol{a} \cdot \boldsymbol{P})} \qquad (2.18)$$

Thus the expression for the total diffracted intensity is

$$|A|^2 = |F|^2 \times \frac{\sin^2(\frac{1}{2}N_x k\boldsymbol{a} \cdot \boldsymbol{P})}{\sin^2(\frac{1}{2}k\boldsymbol{a} \cdot \boldsymbol{P})} \ \mathrm{I} \times \frac{\sin^2(\frac{1}{2}N_y k\boldsymbol{b} \cdot \boldsymbol{P})}{\sin^2(\frac{1}{2}k\boldsymbol{b} \cdot \boldsymbol{P})} \ \mathrm{II} \times \frac{\sin^2(\frac{1}{2}N_z k\boldsymbol{c} \cdot \boldsymbol{P})}{\sin^2(\frac{1}{2}k\boldsymbol{c} \cdot \boldsymbol{P})} \ \mathrm{III} \qquad (2.19)$$

Strong diffraction by the crystal will occur when $|A|^2$ is a maximum, that is when each term I–III is a maximum. It has been shown previously that

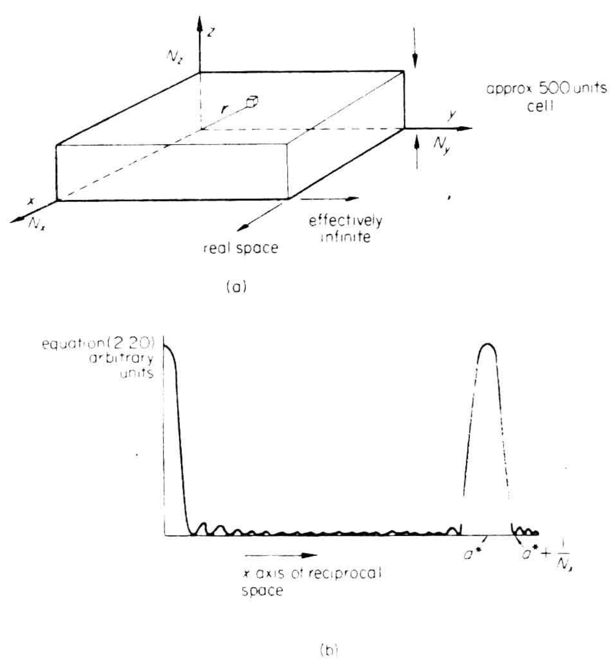

Figure 2.14 (a) The position of the nth unit cell in an electron microscope specimen consisting of N_x, N_y and N_z unit cells in the x, y, z directions respectively. (b) The variation of equation (2.20) along the x axis of reciprocal space

the diffracted wave vector $\boldsymbol{P}$ is a maximum when $\boldsymbol{P}/\lambda = \boldsymbol{g}$. Substituting equation (2.6) into term I of equation (2.19) we have

$$\frac{\sin^2 [\frac{1}{2}N_x k\boldsymbol{a} \,.\, \{\lambda(h\boldsymbol{a}^* + k\boldsymbol{b}^* + l\boldsymbol{c}^*)\}]}{\sin^2 [\frac{1}{2}k\boldsymbol{a} \,.\, \{\lambda(h\boldsymbol{a}^* + k\boldsymbol{b}^* + l\boldsymbol{c}^*)\}]} \quad (2.20)$$

is a maximum if $\boldsymbol{a} \,.\, \{\lambda(h\boldsymbol{a}^* + k\boldsymbol{b}^* + l\boldsymbol{c}^*)\} = h\lambda$ and zero if it is $h\lambda/N_x$. Thus, in effect this term maps the diffracted intensity as a function of position along the x axis of reciprocal space as shown in figure 2.14(b). The fact that the diffracted intensity falls very rapidly to zero on moving a small distance $1/N_x$ from the reciprocal lattice point for a large crystal shows that the reciprocal lattice does indeed consist of an array of points.

2.4 The Reciprocal Lattice and Transmission Electron Diffraction in the Electron Microscope

In most cases electron microscope diffraction patterns are obtained from individual grains and therefore are single-crystal diffraction patterns. They are most easily visualised in terms of the Ewald sphere construction in the reciprocal lattice, but first the reciprocal lattice must be modified to take account of the thin sheet shape of the electron microscope specimen using the results of equation (2.19). It was shown in section 2.3.2 and figure 2.14(b) that the width of the reciprocal lattice point is $2/N_x$, $2/N_y$ and $2/N_z$ in the x, y, z direction. However, the typical electron microscope specimen shown schematically in figure 2.14(a) is a sheet, effectively infinite in its xy plane but finite along the z direction, that is ~500 unit cells thick. Consequently the reciprocal lattice points are very narrow in the z and y directions with intensity distributions of the form shown schematically in figure 2.15(b). In contrast the intensity distribution around the reciprocal lattice points in the z direction is much broader than in the x and y directions owing to the thinness of the sheet, see figure 2.15(a). Consequently the reciprocal lattice points must in fact be treated as streaks parallel to z, the foil normal, see figure 2.15(c). This is equivalent to stating that the Laue condition in the direction z is relaxed and thus a significant diffracted intensity will be obtained even when the Bragg condition is not *exactly* satisfied. The modified Ewald sphere construction which takes account of this is shown in figure 2.16. A vector $\boldsymbol{s}$ is defined describing the deviation from the exact Bragg position when the Ewald sphere cuts the streak. Clearly, as $\boldsymbol{s}$ increases, the diffracted intensity will decrease, see figure 2.16 and if $\boldsymbol{s} \neq 0$ the reciprocal lattice vector is $\boldsymbol{g}' = \boldsymbol{g} + \boldsymbol{s}$.

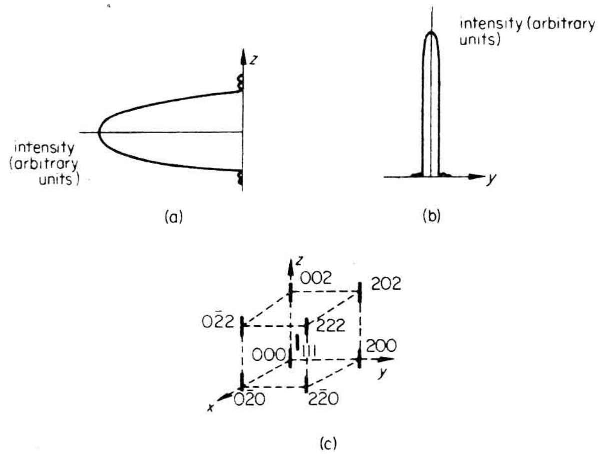

Figure 2.15 (a) and (b) The resulting approximate intensity distribution in reciprocal space parallel to z and y, respectively. The effective streaking of all points in reciprocal space normal to the specimen surface is shown in (c)

The above discussion has important implications for electron diffraction in the electron microscope that can be readily seen with the aid of the Ewald sphere construction in figure 2.17. Here the position of the thin foil is indicated, together with the direction of the incident beam. Although it is only a device to aid interpretation of diffraction

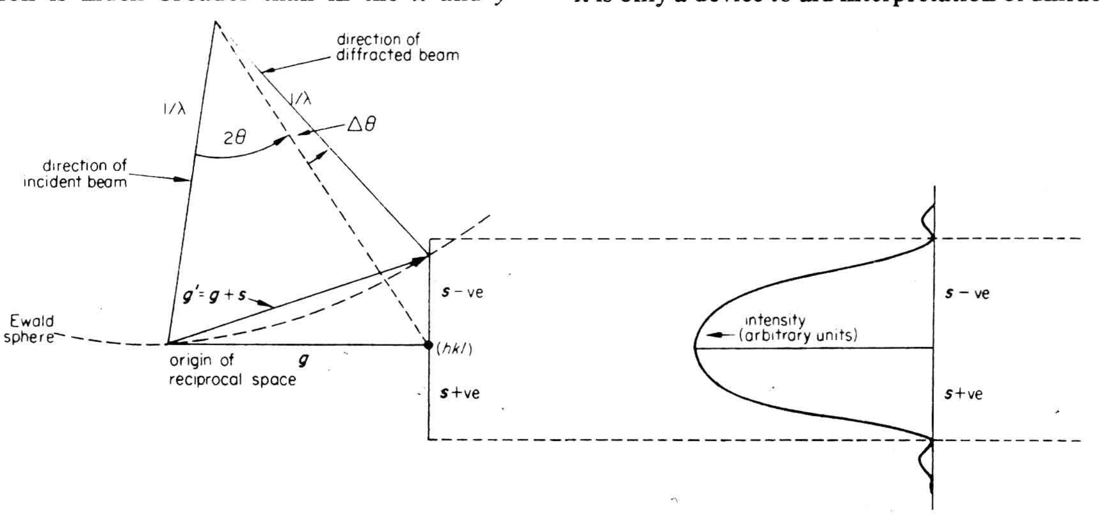

Figure 2.16 The definition of vectors $\boldsymbol{g}$, $\boldsymbol{s}$, $\boldsymbol{g} + \boldsymbol{s}$ in terms of the Ewald sphere construction in reciprocal space